Wavelength and Code Orthogonality Based Distributed Acoustic Sensing over a Passive Optical Network

Pallab K. Choudhury and Élie Awwad
TÉLÉCOM Paris, Institut Polytechnique de Paris (IP Paris), 19 place Marguerite Perey, 91120 Palaiseau, France.
E-mail: elie.awwad@telecom-paris.fr

Abstract: We present a wavelength and code orthogonality based DFOS enabling simultaneous sensing of all paths of a splitter-based passive optical network. Strain sensitivity of $80nm_{pp}$ is measured with no penalty on coexisting 10Gb/s downstream transmission.

1. Introduction

For next generation optical access networks, the central office (CO) needs to manage the typical passive optical networks (PONs) as well as 5G enabled mobile front-haul with several remote radio heads (RRHs) [1]. Recently, telecom operators are much interested in using the deployed fiber cables for sensing purposes, known as distributed fiber-optic sensing (DFOS), to monitor the network's health as well as to explore new business opportunities by aggregating ambient environmental data [2]. In DFOS, a well investigated approach is differential-phase-sensitive optical time domain reflectometry ($\Delta\varphi$-OTDR) in which Rayleigh backscattered (BS) signals are used to measure the dynamic strain along the fiber. However, the operation of CO-based DFOS in PON is not straightforward for two reasons: 1) the BS signals in drop fibers experience additional power loss due to high splitting ratio; 2) the DFOS interrogator receives overlapped BS signals originated from drop fibers of similar lengths leading to branch ambiguity when trying to locate the vibration event. The power loss of BS signals can be minimized by using enhanced-scattering fibers (ESF) [3] or using a reflective semiconductor optical amplifier (RSOA) in optical network units (ONUs) [4]. However, the insertion of ESF in the drop fibers or RSOA in each ONU significantly increases the deployment cost and complexity. On the other hand, branch ambiguity can be avoided by using drop fibers of dissimilar lengths [3] or by maintaining a strict requirement of same lengths along with time-domain-multiplexed ONUs [4]. Overall, both DFOS proposals impose stringent constraints on the lengths of fibers that eventually limit their use in deployed PONs.

Here, we propose a DFOS interrogator capable of interrogating drop fibers simultaneously without any dependency on their lengths, thanks to wavelength and code orthogonality based probe signals that ensure an independent sensing operation over each drop fiber. Moreover, the proposed DFOS interrogator uses optical pulse coding with a correlation step at the receiver side. Compared to conventional high-peak-power single-pulse probing, optical-pulse coding lowers the non-linear interaction between co-propagating sensing and data signals by spreading the transmitted power over time through the used coded sequence. In this investigation, a proof-of-concept experiment is conducted over a simplified PON architecture to sense different events over two branches simultaneously. The results show successful detection of both events with a 16m-spatial resolution up to 600Hz and a strain sensitivity down to $80nm_{pp}$. Moreover, the coexistence of sensing with data transmission is also tested, where a 10Gb/s NRZ-OOK signal is co-propagated along with the sensing signal. The downstream data receiver shows error-free operation even when the optical channel spacing between data and sensing signals is as low as 15 GHz.

2. Proposed DFOS interrogator and its use in PON

Fig. 1(a) shows the architecture of the proposed DFOS interrogator with optical pulse coding. On the transmitter side, a frequency comb is used to generate a number of optical wavelengths for sensing. These sensing wavelengths are distinct from the ones used for data transmission (they can be selected in the same ITU band or a different one), however, a minimum spacing between sensing and data channels is still required. The optical comb is then split in two parts. One part is modulated by a first probing sequence consisting in a binary Golay code, G_1, and the other part modulated by its complimentary sequence G_2, with individual symbols belonging to a BPSK modulation (the case of single-polarization BPSK probing in [5]). The symbol rate is F_{symb} and the probing code duration is T_{code} chosen such as $4T_{rtd} < T_{code} < T_{coh}$ where T_{rtd} is the round-trip delay over the longest sensed fiber branch and T_{coh} is the coherence time of the light source [5]. The modulated signals are de-multiplexed through two WDM filters leading to N sensing channels λ_{s1}, λ_{s2}..... λ_{sN} that are orthogonal to each other in wavelength and codes (stemming from the complementary nature of the used sequences). On the receiver side, the backscattered signals coming back from the optical fiber are first de-multiplexed. Then, a dual-polarization coherent receiver is used in self-homodyne configuration to capture the backscattered optical field and project it over two polarization states to reduce polarization fading. Depending on the bandwidths of the comb and the photodiodes, several pairs of balanced photodiodes and local oscillators (filtered from the comb) can be used.

After sampling the photocurrents and reconstructing the complex envelope of the BS signal, the signal from each

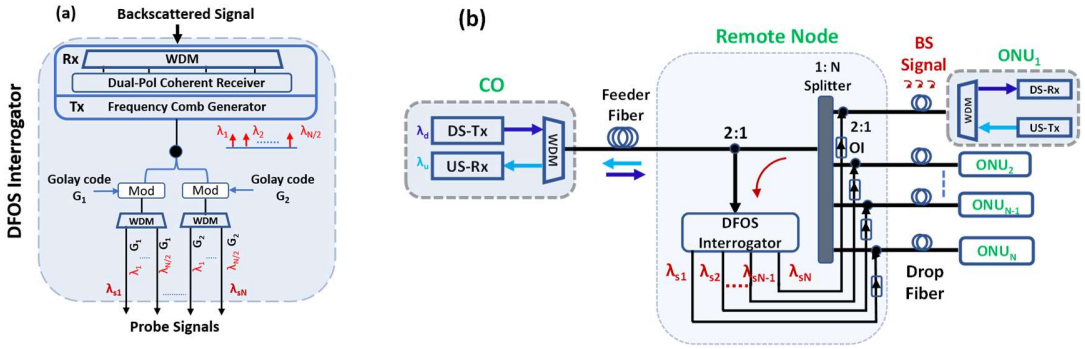

Fig. 1 a) Proposed DFOS interrogator; b) DFOS interrogator for a PON with coexistence of data and sensing signals.

sensing wavelength can be extracted and correlated with the original probing sequence (G_1 or G_2) to find the estimates of the channel response of the sensed fiber (space-time series of 1×2 matrices, given the single-polarization emission and dual-polarization reception at the interrogator), from which the evolution of the temporal optical phase along the fiber is extracted. Since any strain variation over the fiber linearly changes the optical phase, by differentiating the spatially cumulated phase terms, the phase variations can be estimated and located, with a gauge length $S_r = v_f/(2.F_{symb})$ and acoustic bandwidth BW$= 1/(2T_{code})$ where v_f is the velocity of light in the fiber.

Fig. 1(b) shows a use case of the proposed DFOS interrogator in PON where the goal is to simultaneously detect vibrations over N drop fibers after a power splitter. The scheme shows no changes at existing ONUs, thus end-users' premises are unaffected. Downstream (DS) and upstream (US) data channels use wavelengths λ_d and λ_u with DS and US transceivers in CO and ONUs. The DFOS interrogator is placed at the remote node (RN) where sensing channels use $N/2$ separate wavelengths λ_s modulated by one of the probing sequence (G_1 or G_2) and leading to N probes. Each unique combination of λ_s and probing code is assigned to one drop fiber after the 1:N splitter through a 2:1 coupler and an optical isolator (OI). Backscattered signals from the drop fibers go through the splitter and are merged into the receiver of the DFOS interrogator where the WDM filter only keeps the sensing channels. The DFOS interrogator performs the correlations as described earlier to retrieve the sensing information from the N branches simultaneously.

3. Proof-of-concept experiment

An experimental setup emphasizing on code orthogonality is shown in Fig. 2(a) with two 3km-long branches. A 1kHz-FWHM-linewidth laser at 1550 nm is used as a single sensing laser source with an output power of 11dBm. 90% of the light is then split in two halves that go through two intensity modulators, and 10% is used as local oscillator for the dual-polarization coherent receiver. Two complementary Golay signals (G_1 and G_2) are generated by an arbitrary waveform generator to drive two MZMs biased at their null point to generate BPSK signals. For both, F_{symb} =50 Mbit/s and T_{code} = 0.16ms yielding a gauge length of 2.05m and a maximum acoustic bandwidth of 3kHz. Each modulated signal is then amplified and transmitted over SSMF fibers through an attenuator and an optical circulator (OC). The attenuator controls the optical power at the fiber input to study the tolerance of the DFOS scheme to optical loss. Two piezoelectric fiber stretchers (PZS) are used to create dynamic strains on the fiber branch-1 (B-1) and branch-2 (B-2) at 1km and 3km from the remote node respectively. PZS-1 and PZS-2 are driven by two sinewaves of frequencies 400 and 600Hz and peak-to-peak voltages 30 and 20mV, yielding fiber expansions of 120 and 80nm$_{pp}$, respectively. Finally, BS signals from the two branches go through the OCs and to a dual-polarization coherent receiver through an optical coupler. Four balanced photodiodes (ThorLabs PDB480C) and a 4-channel oscilloscope (Tektronix DPO72004B) capture the full complex-envelope of the BS signals at 250 MS/s over 40ms. During this

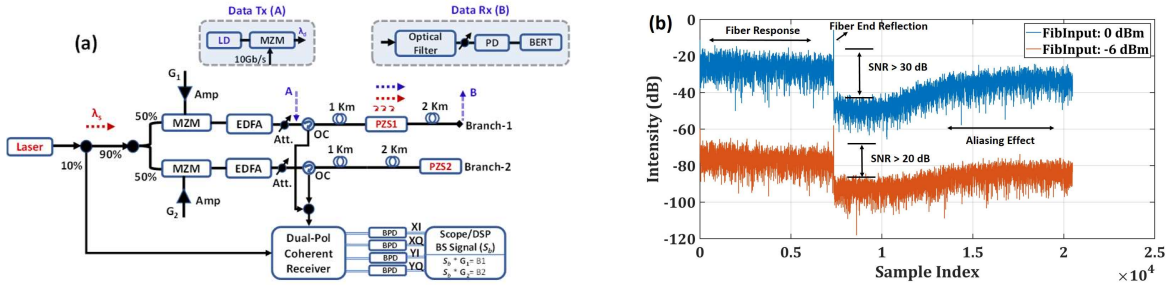

Fig. 2 a) Experimental setup; b) Intensity responses of BS signal of branch B1 for two different fiber input power values.

acquisition, the two branches are continuously and periodically probed every T_{code}. Even though the BS signals from B-1 and B-2 occur at the same wavelength, the corresponding fiber responses of B-1 and B-2 can be separated by correlating the detected signal with each of the orthogonal probing codes G_1 and G_2. In static conditions, two optical powers at the fiber input are tested: 0 and -6 dBm, generating average BS signal at the coherent receiver input of -39 and -45dBm respectively. For both power levels, the receiver successfully recovers the fiber responses as shown in Fig. 2(b) for branch B-1 with SNR levels 30 dB and 20 dB above the noise level respectively, indicating that the coherent receiver is capable of operating with very low levels of BS signals.

Fig. 3(a) shows the BS intensities of B-1 and B-2 estimated from the coded sequences. We can see the fiber responses in the first part followed by an aliasing pattern. Then, the standard deviations (Std) of the differential phases are computed for both B-1 and B-2 in a subset of high-reflecting fiber segments (every 8 segments) leading to an average resolution of 16m. Fig. 3(b) show two strong Std peaks at the locations of the PZSs, at 1km and 3km, clearly demonstrating the identification of both events over the corresponding branch simultaneously. Fig. 3(c) and (d) show the time evolution of the estimated differential phases at the event locations and at neighboring positions. The measured peak-to-peak phase amplitudes are 1.17 and 0.78rad$_{pp}$ respectively. Knowing that optical phase variations are linked to fiber extensions dL through $d\varphi = dL.4\pi n\xi/\lambda$, where ξ= 0.78 is the photo-elastic scaling factor and n the refractive index of the fiber core, the measured phase variations are quite close to the theoretical expected ones for dL = 120nm$_{pp}$ and 80nm$_{pp}$ (1.14 and 0.76rad$_{pp}$ resp.). We can also see that phase variations in neighboring positions are much lower as expected. Fig. 3(e) shows the power spectral density (PSD) of the estimated differential phases at the event locations, which clearly indicate 400Hz and 600Hz tones with an SNR> 30dB.

Finally, we investigate the performance of a DS transmission at 10Gb/s using NRZ-OOK along with the sensing signal over B-1. The data Tx consists of a tunable laser and an external modulator driven by a PRBS sequence. The modulated data signal is inserted at point A, as shown in Fig. 2(a), through a coupler. The data Rx is placed at point B and consists of a tunable optical filter (Yenista XTA-50, FWHM~15GHz), a 12.5GHz-bandwidth PIN photodiode) and a Bit Error Rate tester. When the sensing signal is turned off, the sensitivity of the data Rx is adjusted to get a BER=10^{-9} and is then maintained at the same level. Then, the sensing signal is turned on and the BER of DS data is measured, over several minutes, against various channel spacing between data and sensing signals. The results in Fig. 3(f) show no significant performance degradation of DS data even when the spacing is as low as 15GHz, indicating no nonlinear interaction of signals during the propagation over the fiber. The insets of fig. 3(f) show the eye diagrams at 15GHz and 10GHz spacing as well as an optical spectrum at point A for a 15GHz spacing.

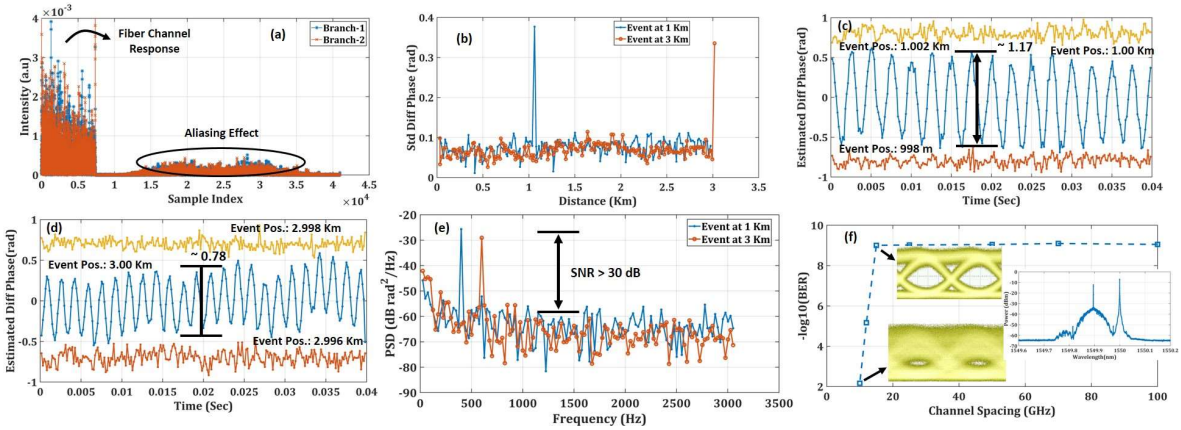

Fig. 3 a) Estimated channel responses with correlation noise; b) Standard deviations of differential phases against fiber distance; c) & d) Estimated phases around the events; e) PSD of estimated phases at the locations of events; f) BER of co-propagating 10Gb/s DS NRZ-OOK data versus channel spacing (insets show eye diagrams and optical spectrum).

4. Conclusions

We proposed and demonstrated a DFOS interrogator for splitter-based PONs that removes branch ambiguity. Also, the used pulse-coded sensing channel showed no impact on the BER of a DS data channel when they are 15GHz apart.

5. References

[1] F. Saliou et al., "Coexistence in future optical access networks from an operator's perspective," *J. Opt. Comm. Netw.* 16, A78-A88, 2024.
[2] L. Palmieri, et al., "Rayleigh-based distributed optical fiber sensing", *Sensors*, *22* (18), p.6811, 2022.
[3] B. Zhu, et al., "Distributed Acoustic Sensing over Passive Optical Networks Using Enhanced Scatter Fiber", *OFC*, paper M1K.1, 2024.
[4] Y. Huang, et al., "Simultaneous Optical Fiber Sensing and Mobile Front-Haul Access over a PON", **OFC**, paper Th1K.4, 2020.
[5] C. Dorize et al., "Enhancing the performance of coherent OTDR systems with polarization diversity complementary codes," *Opt. Exp.* 26, 2018.